

Aberration coefficients of multi-element cylindrical electrostatic lens systems for charged particle beam applications

Omer Sise*, Melike Ulu, Mevlut Dogan

Department of Physics, Science and Arts Faculty, Afyon Kocatepe University, 03200 Afyonkarahisar, Turkey

Received 8 September 2006; received in revised form 1 November 2006; accepted 2 January 2007

Available online 12 January 2007

Abstract

In order to analyze the imaging properties of an electrostatic lens system, it is necessary to know how various sources of aberration combine to increase the size of final image or spot. In this paper, we investigated the spherical and chromatic aberration coefficients of multi-element electrostatic lens systems as a function of the lens voltages and magnification, using the electron ray tracing simulation programs SIMION and LENSYS. These programs can be used to obtain electron optical aberration integrals which involve the axial potential distribution and its derivative, and two independent trajectories and their derivatives for the determination of the third- or fifth-order aberration coefficients of multi-element lenses. Optical simulation of the intensity distribution has quantitatively shown that the aberration in the crossover image causes an electron beam blur and a positioning error on the focus spot. If a high positive voltage with respect to the first element's potential is applied to the lens elements, the aberrations as well as the minimum beam divergence can be reduced. The reason, obtained from numerical simulation, is that a positive voltage increases the electron velocity, shortening the electron drift time across the region with aberrant field.

© 2007 Elsevier B.V. All rights reserved.

PACS: 41.85.Ne

Keywords: Electrostatic lenses; Multi-element lenses; Electron optics; Zoom lens; Aberration coefficients; SIMION and LENSYS

1. Introduction

In the development of charged particle optical instruments, such as electron or ion guns, lithography systems, energy analyzers, time of flight spectrometers, electron microscopes, it is necessary to determine the performance of the system and to fabricate lenses and apertures taking into account the aberration effects. It is well known that the effects of aberrations cause degradation of the focused beam spot and thereby severely restrict the spatial resolution of the system. The main part of this limitation arises from the spherical C_s and chromatic C_c aberrations, which are the principal aberrations and relatively large compared to optical lenses, that adversely affect the focusing properties of electrostatic lenses. Therefore, it is highly desirable to design multi-element electrostatic lenses

with small spherical and chromatic aberration coefficients in order to obtain high resolution.

The calculation of the third-order aberration coefficients using integrating functions of the axial potential distribution is available in the literature. There are also many excellent books on charged particle optics in general as well as more specific books on aberration coefficients that cover much useful material [1–8]. Brunt and Read [9] have investigated the effects of the third-order spherical aberrations of electrostatic lenses for different operating conditions and pupil positions, and showed that the radius of disc of least confusion can be reduced by moving the Gaussian image plane to the fixed plane at a fixed voltage ratio. Renau and Heddle [10,11] developed a computer model to calculate the potential distribution of a two-element lens using a variational method, and described the theory of the model to calculate the third- and fifth-order aberration coefficients. The applicability of the Renau and Heddle approximation was investigated by Martinez and

*Corresponding author. Tel.: +90 2722281311; fax: +90 2722281235.
E-mail address: omersise@aku.edu.tr (O. Sise).

Sancho [12] and it has been shown that for the weaker lenses this approximation is excellent and fails when the lens becomes stronger. The aberration coefficients of two- and three-element lenses have been investigated by Szilagy and co-workers [13–15] for various diameters, gaps and voltage ratios with special focusing characteristics.

It is well known that in the absence of space charge, spherical aberration of rotationally symmetric electrostatic lenses cannot be avoided [16]. To overcome the spherical aberration in electrostatic lenses, several correction methods have been developed. A typical method to reduce aberration is that of using electrostatic multipoles, the so-called quadrupole and octupole lenses. In this method, the third-order spherical aberration can be reduced by applying an accelerating potential to some lenses of a quadrupole system. Dowker et al. [17] also showed that the middle element of a three-element lens can be split into four quadrants to provide lateral deflection. Baranova et al. [18–20] later presented a comparative study of chromatic and spherical aberrations in the quadrupole–octupole type for multi-element lenses, and it has been shown that the third-order aperture aberration can be eliminated. Recently, an electrostatic corrector composed of lens elements that are rods with hemispherical ends have been designed by Baranova et al. [21] for low-voltage scanning electron microscopes.

On the other hand, Kato and co-workers [22–24] have shown that the spherical aberration of electrostatic lenses can be corrected for the aperture angle of up to 60° by introducing spherical mesh. They also demonstrated that the use of an ellipsoidal mesh provides remarkable performance characteristics for electrostatic lenses. Recently, Uno et al. [25] described a procedure for the automatic aberration correction in scanning electron microscopy using an image processing technique, and succeeded in incorporating a stable system into a general purpose.

In order to make aberration analysis simple and concise with high accuracy, several methods have been carried out for electron lenses, and nearly all of them are based on either aberration integrals [26], ray tracing [27], or differential algebraic methods [28]. Also, many computer programs, such as SIMION [29], LENSYS [8], and CPO [30], have been developed for solving problems in charged particle optics. These programs are more useful because they can be used to compute overall aberrations in the lens.

Rotationally symmetric electrostatic lenses have been commonly used in electron spectrometer instruments, such as electron guns and entrance optics of electron energy analyzers. In a recent paper, we presented the focal and zoom-lens properties of several kinds of multi-element cylindrical electrostatic lens systems [31]. The purpose of the present work is to give a systematic presentation of the spherical and chromatic aberrations of multi-element lenses and to investigate their effects on the intensity distribution of the final spot. Making plots of the aberration coefficients as a function of the lens parameters

is potentially useful for electron spectroscopy, for instance, in coincidence spectroscopy [32].

We used SIMION and LENSYS packages, ray-tracing programs, which solve the Laplace equation by a finite difference approach for a given geometry of electrodes with fixed voltages to get a potential array. In this work, it will be shown that direct ray-tracing provides an accurate and useful tool for the analysis of high order aberrations in electrostatic systems. In SIMION, electron trajectories were simulated for the resulting potential using ten points per millimeter resolution to reproduce the shape precisely [33]. Randomized electron packages with starting parameters were also used for the simulations of intensity distribution.

2. Aberration coefficients

In designing lens systems it is more important to know the relationships between the aberration coefficients and the corresponding lens parameters, such as focal lengths and magnification. One type of aberrations for lenses is spherical aberrations, where the outer zones of the lens focus more strongly than the inner zones. The representation of spherical aberration effect for a two-element lens is shown in Fig. 1a for three different angles. The spherical aberration can be characterized by the third-order coefficients C_s defined by the relation [8]

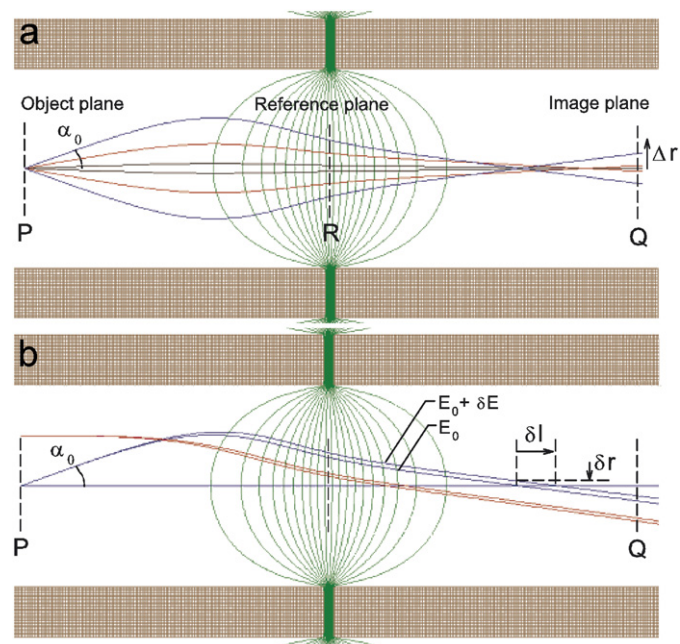


Fig. 1. (a) Representation of the spherical aberration of an image for a given object distance P and voltage ratio $V_2/V_1 = 20$ in a two-element lens. Here, R is the reference plane of the lens and Q is the Gaussian image plane. The radius of the spherical aberration disc is Δr at the plane Q . α_0 is the maximum half angle of the pencil of rays making up the object. (b) Representation of the chromatic aberration. The lower ray of each pair has the correct energy to form an image and the other rays, which have a slightly higher energy, cross the image plane at points which are displaced from the image plane.

$$\Delta r = -MC_s \alpha_0^3 \quad (1)$$

where Δr is the radius of the disc formed in the Gaussian image plane by non-paraxial rays starting from an axial object point with a maximum half angle α_0 , and M is the linear magnification. The image blur in this plane is usually called the disc of least confusion (see for example, Refs. [4,8]). Brunt and Read [9] also showed that the radius of disc of least confusion is smaller than the radius at the Gaussian image plane (approximately by a factor of 4) and that disc is situated in front of it. Another type of aberrations is chromatic aberrations, where charged particles of slightly different energies get focused at different image plane. The coefficient of chromatic aberration C_c is defined by

$$\delta r = -MC_c \alpha_0 \frac{\delta E}{E_0} \quad (2)$$

or can be expressed in terms of $\delta \ell$ to illustrate the non-dependence of the chromatic aberration coefficient on the angle α_0 . Fig. 1b shows the four pairs of rays through a two-element lens for different initial conditions. We assumed that one ray with energy E_0 crosses the axis at the image point, the higher energy ray with $E_0 + \delta E$ crosses the axis at a distance $\delta \ell$ beyond this point and at a distance δr above the axis (Note that we cannot ignore the effects of spherical aberration for large angles to illustrate chromatic aberration as shown in Fig. 1b). According to these equations, both types of aberrations can be minimized by reducing the convergence angle of the system so that the charged particles are confined to the center of the lenses.

3. Trajectory simulations

Aberration coefficients of electrostatic lenses can be written as a polynomial in reciprocal magnification and the expression for the coefficients occurring in these poly-

nomials are likewise available:

$$C_s(M) = C_{s0} + C_{s1}M^{-1} + C_{s2}M^{-2} + C_{s3}M^{-3} + C_{s4}M^{-4} \quad (3)$$

$$C_c(M) = C_{c0} + C_{c1}M^{-1} + C_{c2}M^{-2}. \quad (4)$$

To evaluate C_{si} and C_{ci} coefficients of cylindrical symmetric lenses one can use the methods described by Harting and Read [4] and Heddle [8] by using the integral representation of the aberration coefficients. Fig. 2 shows an example of the separate integral equations of C_{si} obtained from ray-tracing simulations together with the potential distribution for the case of a two element lens with an acceleration voltage ratio 1 : 18.25. Each integral, being functions of only the electrode geometry and potentials, is written as the product of terms involving the $T = V/V'$ parameters (where V is the axial potential (see Fig. 2) and V' its derivative), which are the same for all

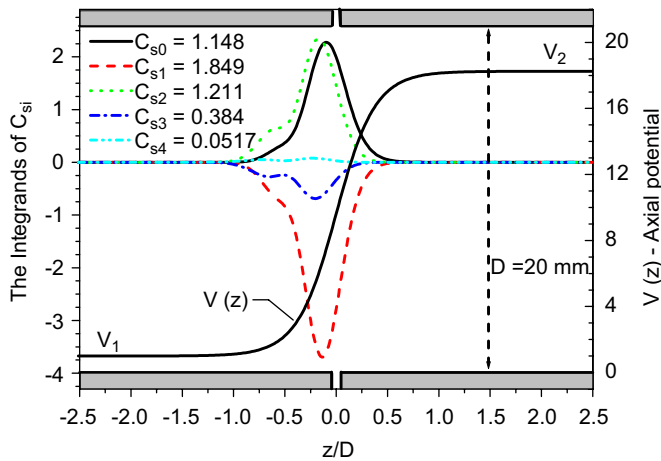


Fig. 2. The integrands for each spherical aberration coefficients C_{si} and axial potential $V(z)$ for a two-element lens with an acceleration voltage 1 : 18.25 for $P/D = Q/D = 2$. The individual curves can readily be associated with particular coefficients and for this lens they are, from the top, C_{s0} , C_{s2} , C_{s4} , C_{s3} , C_{s1} .

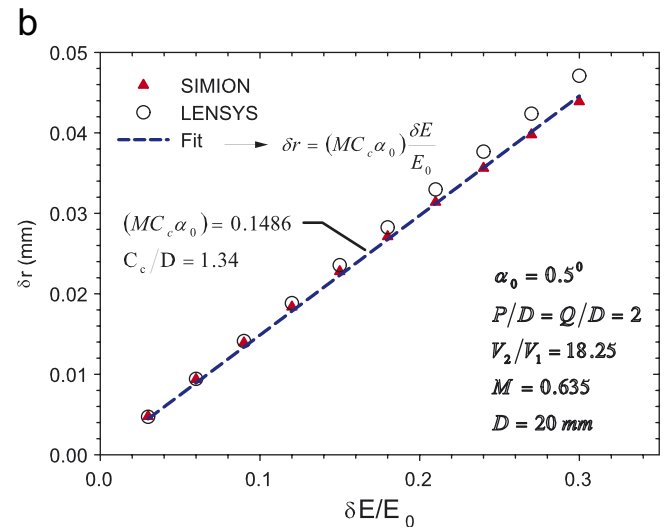
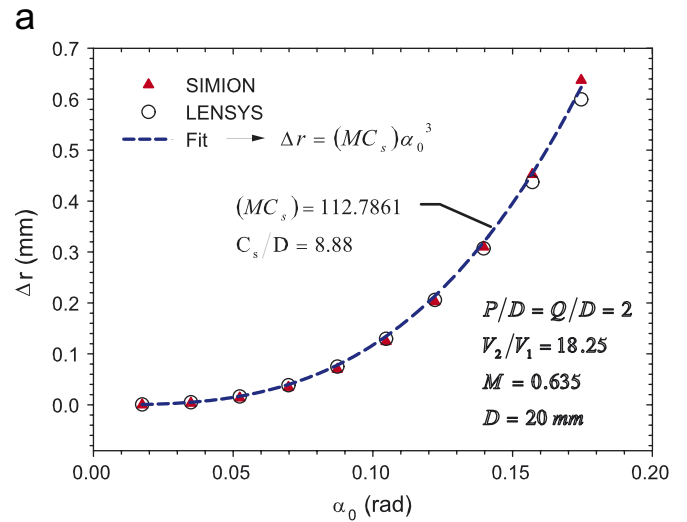


Fig. 3. Calculations of the aberration coefficients C_s and C_c of a two-element lens for $P/D = Q/D = 2$ and $V_2/V_1 = 18.25$ using the ray-tracing simulation programs SIMION and LENSYS. The aberration discs Δr and δr are recorded as a function of α_0 and $\delta E/E_0$, respectively.

applications of the lens. In the symmetric case (einzell or unipotential electrostatic lenses) the number of independent aberration coefficients is reduced to either three for spherical aberration where $C_{s0} = C_{s4}$ and $C_{s1} = C_{s3}$ or two for chromatic aberration where $C_{c0} = C_{c2}$ [34].

Theoretically there is no difference between electron optics and ion optics (except differences in mass and sign of charge) and a more suitable generic term would be “charged particle optics”. Here we used electrons in simulations, but the lens systems can also be used to focus

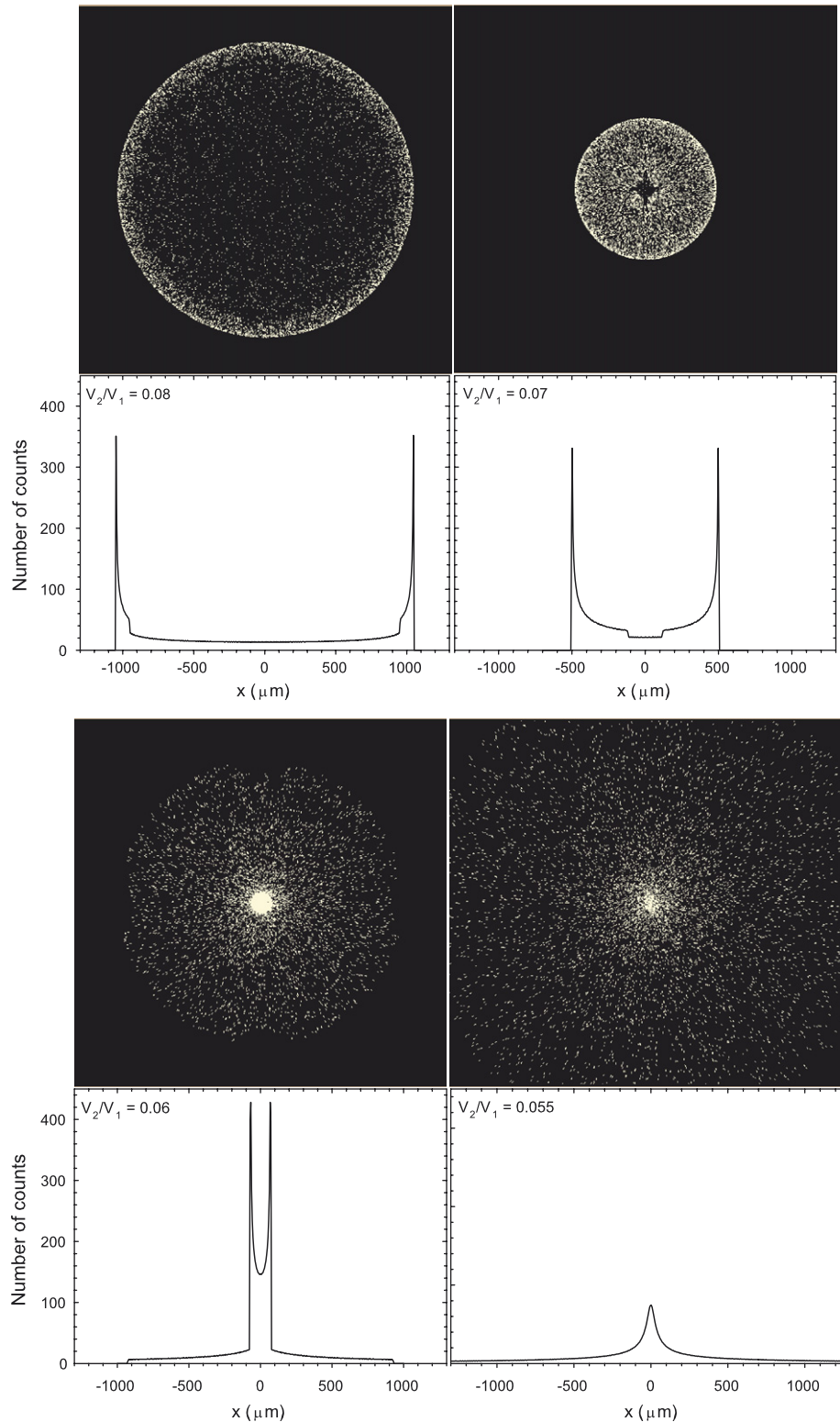


Fig. 4. Distribution of electrons at a fixed image distance for a two-element lens with $P/D = Q/D = 2$ for four different voltage ratios, $V_2/V_1 = 0.08$, 0.07, 0.06 and 0.055 (see text). The optimal focus point corresponds to the case for $V_2/V_1 = 0.06$.

positive ions with all the voltages reversed in sign. Briefly, for conventional charged particle optics, spherical and chromatic aberration refer to the notion that particles with different initial velocity angles with respect to the optical

axis and different initial speeds are not exactly mapped on one point, but on a disk in the image plane. In order to find the aberration coefficients C_s and C_c , the aberration discs Δr and δr are recorded as a function of α_0 and $\delta E/E_0$,

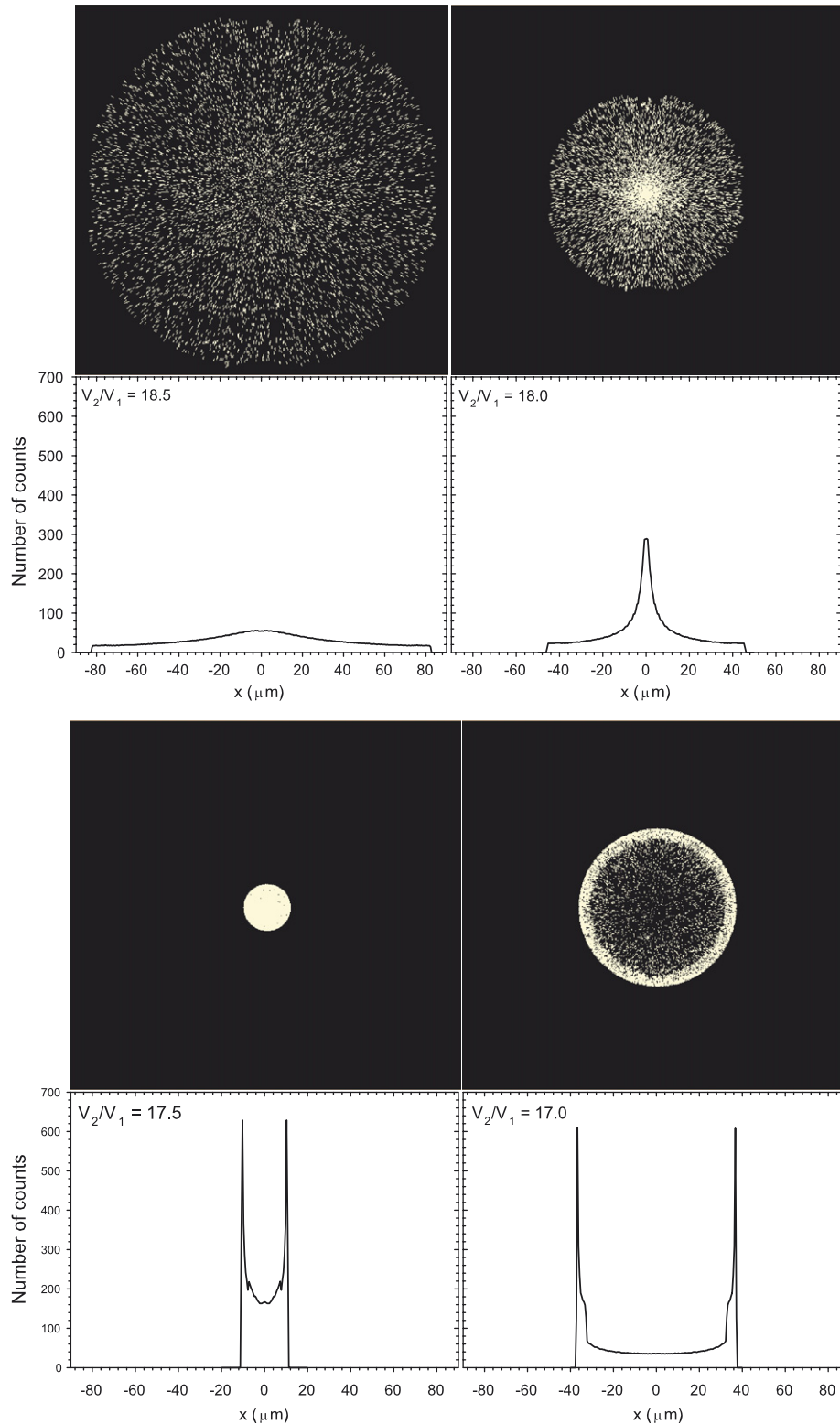
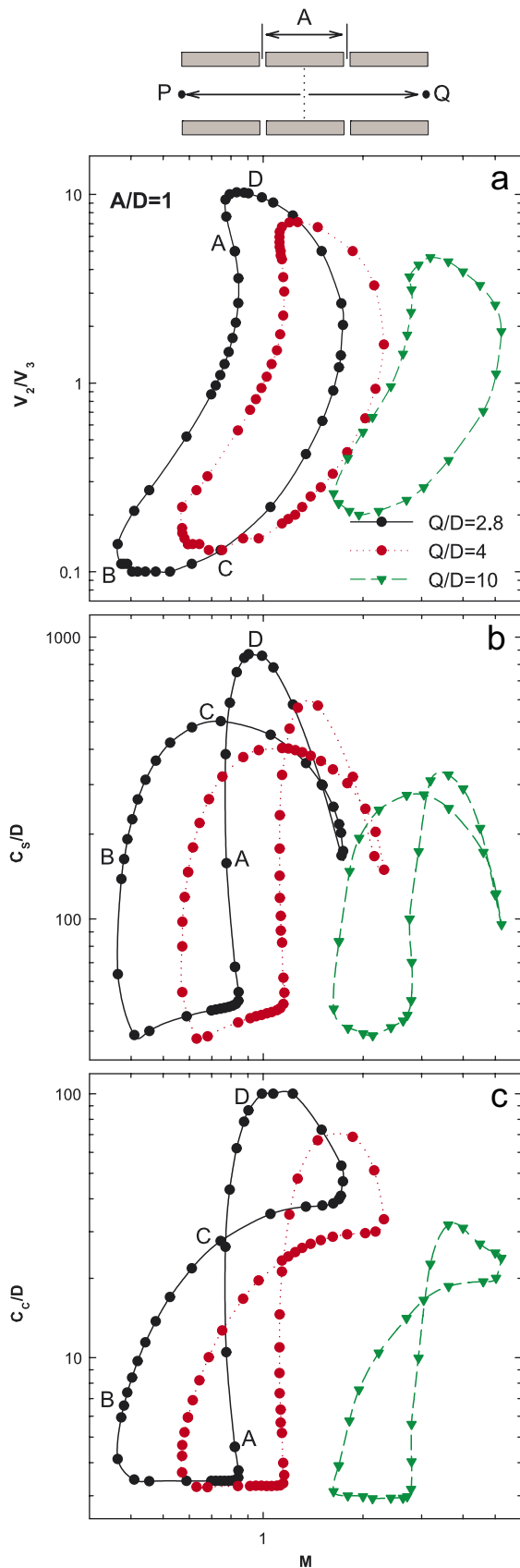


Fig. 5. Distribution of electrons at a fixed image distance for a two-element lens with $P/D = Q/D = 2$ for four different voltage ratios, $V_2/V_1 = 18.5$, 18.0, 17.5 and 17.0 (see text). The optimal focus point corresponds to the case for $V_2/V_1 = 17.5$.



respectively, as shown in Fig. 3. This figure shows the procedure for obtaining C_s and C_c using SIMION and LENSYS. These coefficients have been evaluated for various lens configurations, both for the decelerating and accelerating lens voltages, and for three-, four- and five-element electrostatic lenses. All voltage values applied to lens electrodes are on the basis that $V_1 = 1$ V and so V_n represents V_n/V_1 . The first electrode is placed at the same potential (1 V) with respect to the electrons primary energy ($E_0 = 1$ eV). The object and image distances, P and Q , were determined easily as well as the focal lengths by difference. The linear magnification M was determined by the ratio of final to initial beam diameter in the radial axis, $r_{\text{image}}/r_{\text{object}}$, respectively.

4. Results and discussion

4.1. The effects of aberrations on the final spot

The calculation of the aberration coefficients allows us to consider in which way charged particles are affected by the spherical and chromatic aberration. A simple estimate of the aberrations in a lens can be found if it is assumed that the beam emanates from a single source point (P) and is to be focused to a single image point (Q). In order to see the effects of the spherical aberrations, electrons with different initial properties are traced through the lens and the final spot size dependence on exit radial displacement is monitored. This is carried out by varying the incoming semi-angle α . For chromatic effects, naturally, spot size dependence on beam energies needs to be considered. Graphs of the simulation predicted the intensity distribution of the final spot dependence on the radial exit displacement for a two-element lens are presented in Figs. 4 and 5 for $P/D = Q/D = 2$ and both for accelerating and decelerating lens. The semi-angle is varied between 0 and $\pm 4^\circ$. It is enough to consider a large number N (15,000) of incoming electrons in a SIMION simulation where the angle α can be randomly varied. Here, this angle has been chosen to be 4° in order to clearly show aberrations. Spot diagrams of the kind shown in these figures were obtained for cases likely to be of importance for electron microscopy [35].

Harte [36] and Brunt and Read [9] have discussed already that there is no single focus point beyond the paraxial approximation, and that for an incoming ray with an angle α as shown in Fig. 1a. If we put a position sensitive detector (PSD) after the two-element lens perpendicular to the optical axis, we would observe a spot of beam of finite

Fig. 6. (a) The variation of V_2/V_3 which contains two voltage ratios, (b) the spherical, and (c) chromatic aberration coefficient, C_s/D and C_c/D , of the three-element zoom lens as a function of the magnification for various image distances Q/D , 2.8 (●), 4 (▼) and 10 (■) and for $P/D = 3.5$. There are four pairs of values of V_2/V_1 and V_3/V_1 which satisfy the focusing condition: AB: $V_2/V_1 > 1$ and $V_3/V_1 > 1$; BC: $V_2/V_1 > 1$ and $V_3/V_1 < 1$; CD: $V_2/V_1 < 1$ and $V_3/V_1 < 1$; DA: $V_2/V_1 < 1$ and $V_3/V_1 > 1$ (see Fig. 7 of Ref. [31] for voltage ratios).

(not zero) size. The size of this spot depends on both the focusing voltage V_2/V_1 and the position of the PSD. We could define operationally the optimal focusing voltage of the lens where one has to calculate V_2/V_1 in such a way that the observed spot of beam presents the minimum size, i.e. with the smallest average distribution of electron beam. Let us consider a voltage ratio $V_2/V_1 = 0.08$ in Fig. 4. It is clear that the spot of the beam is large simply because the rays of electrons have not converged yet. If we increase the strength of the lens (as in case $V_2/V_1 = 0.07$), some of the rays have converged already and the size of the spot decreases. If we change the voltage ratio a little bit (case $V_2/V_1 = 0.06$) the size of the spot decreases even more. However, case $V_2/V_1 = 0.06$ precisely corresponds to the critical voltage of the lens where the smallest spot of beam is obtained, and thus the optimal focusing voltage, because if we continue changing V_2/V_1 with a small variation, the rays coming from the object distance with a maximum half angle $\pm\alpha_{\max}$ are now farthest from the optical axis, producing a larger spot of beam, as in case

$V_2/V_1 = 0.055$. The simulations of the intensity distribution for the accelerating lens is also presented in Fig. 5, which are the same as in the case of the decelerating lens. It is clearly seen that the focus is confirmed to be at $V_2/V_1 = 0.06$ and 17.5. However, the latter case (accelerating voltage) is more desirable considering the lower aberration disc.

We have addressed the problem of finding the focusing voltage for which the spot of the electron beam has the minimum size. This voltage is then defined as the optimal focusing voltage. Similar distributions of the beam was obtained by Milosavljevic et al. [37] with changing the focusing voltage that was partly a consequence of spherical aberrations. Although the results shown in Figs. 4 and 5 are obtained for a particular example, the shapes of the different spots are rather general for chromatic aberration effect. The distribution of electrons at a fixed image distance serves to evaluate the magnitude of aberrations for an electron optical system. This direct determination is much more convenient than an evaluation based on the

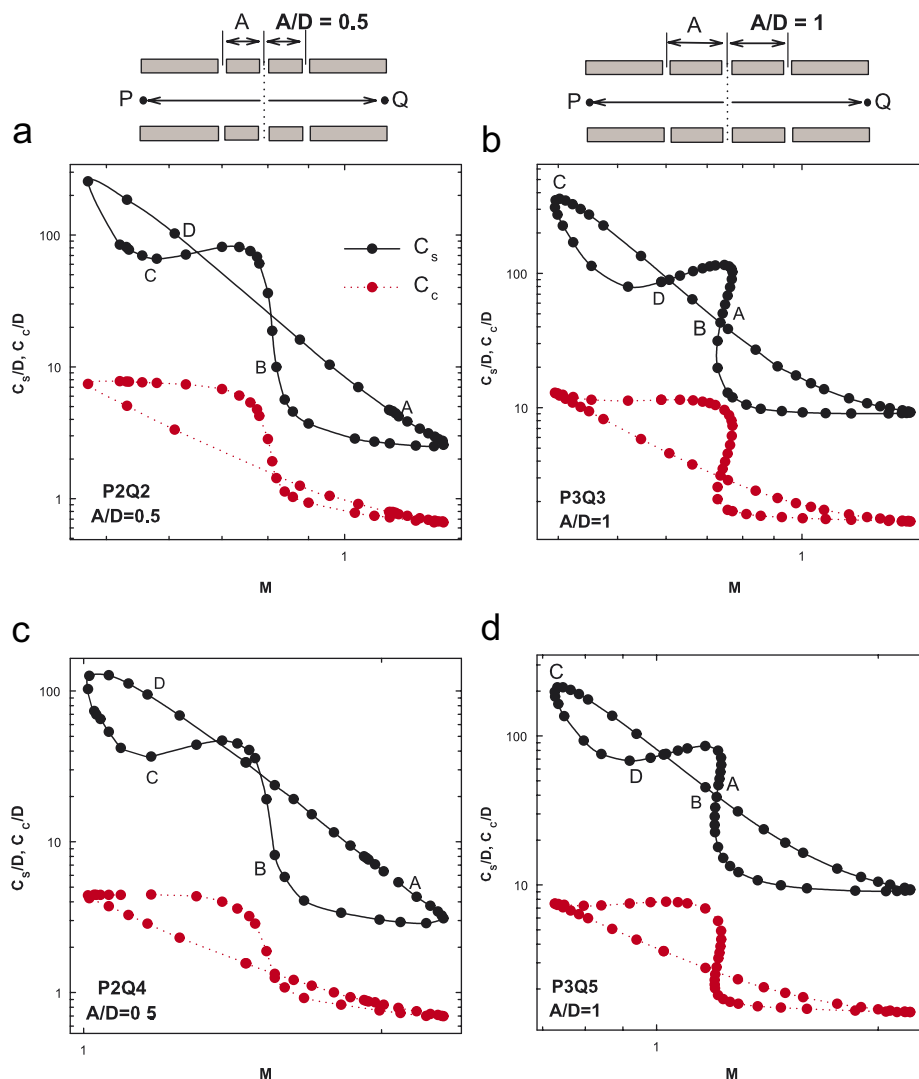


Fig. 7. Values of the spherical and chromatic aberration coefficient C_s/D and C_c/D for four-element lenses with (a)–(c) $A/D = 0.5$ and (b)–(d) 1 as a function of the magnification for different values of P and Q (see Fig. 8 of Ref. [31] for voltage ratios).

classical aberration coefficient defined at the Gaussian image plane. The determination of the optimal focus point (or optimal voltages) of an electrostatic lens is of fundamental importance in many electron optical systems, such as in electron spectrometer instruments.

4.2. Three-element lenses

Fig. 6 (top) shows sections through the three-element lens system that we have studied. The lens consists of three coaxial cylinders of the same diameter. Expressing all the dimensions in terms of the inner diameter D , the gaps between the cylinder are $G = 0.1D$, and the distance between the midpoints of the gaps is $A/D = 1$. For a given three-element lens, there are four pairs of values of V_2/V_1 and V_3/V_1 which satisfy the focusing condition in the image plane (AB: $V_2/V_1 > 1$ and $V_3/V_1 > 1$, BC: $V_2/V_1 > 1$ and $V_3/V_1 < 1$, CD: $V_2/V_1 < 1$ and $V_3/V_1 < 1$, DA: $V_2/V_1 < 1$ and $V_3/V_1 > 1$). The spherical and chromatic aberration coefficients of the three element lenses have been calculated for both accelerating and decelerating lenses. It is well known that the aberration coefficients, C_s and C_c , for three-element lenses with the higher values of V_2/V_1 are always less than the lower values [38]. This is because the accelerating lens serves the purpose of reducing the angular spread of the electron beam and pencil angles, and the paths of charged particles with the higher values of V_2/V_1 in the center of the lens are much closer to the axis.

Since the aberration coefficients strongly depend on the magnification, one wishes to know the dependencies of the quantities C_s and C_c on M . Fig. 6 illustrates the zoom-lens properties of the lens in this way. Here, for consistency, we use the same values of voltage ratios as in Ref. [31] to calculate the aberration coefficients. If the lens is operated with $V_2/V_3 > 1$ the magnification M changes by a small amount from 0.74 to 0.88 for $Q/D = 2.8$ when the ratio of final to initial energy (V_3/V_1) is changed from 8 to 1.2, where V_2 is altered to keep the image position constant. The four possible configurations lead to significantly different coefficients of spherical and chromatic aberration for all values of the magnification. With its low spherical and chromatic aberration and small change in magnification this is obviously the better mode in which to operate the zoom lens as a variable acceleration system. If it is desired to vary magnification then the outer mode of operation in which the center electrode is at a low voltage can be used, although this mode has inherently higher spherical and chromatic aberration. It was shown that for all values of the magnification, the spherical and the chromatic aberration coefficients were least for AB mode.

4.3. Four-element lenses

Many different types of geometry and operating conditions of four-element lenses are of interest [39], but in this part we have used two representative geometries $A/D =$

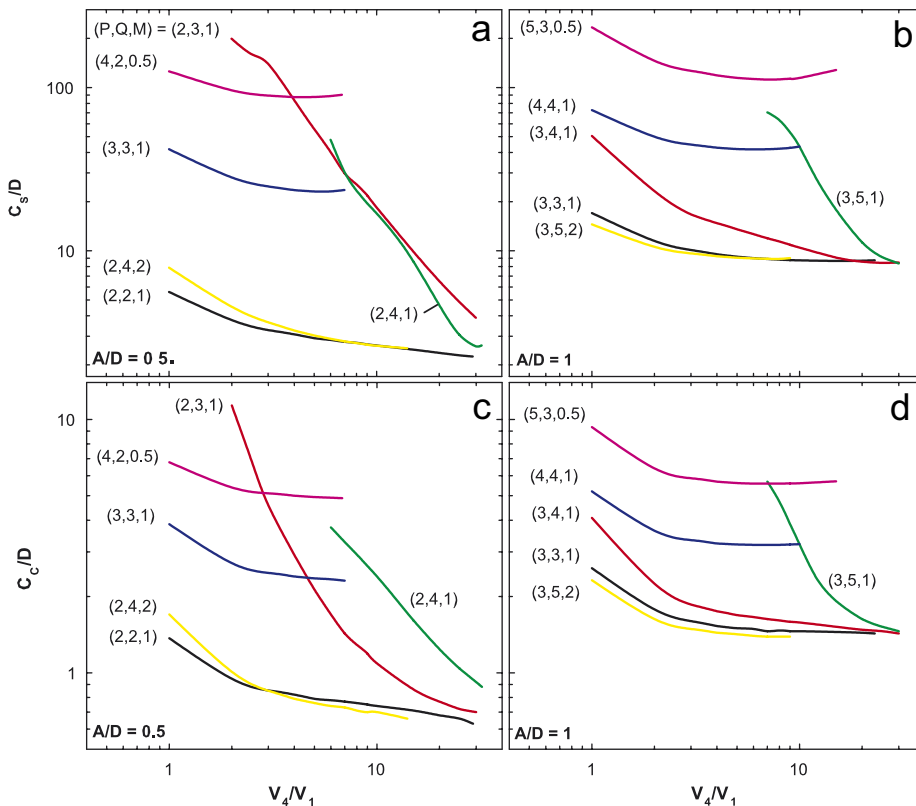


Fig. 8. Values of the (a)–(b) spherical and (c)–(d) chromatic aberration coefficient C_s/D and C_c/D for four-element lenses with $A/D = 0.5$ and 1 as a function of V_4/V_1 for six combinations of (P, Q, M) (see Fig. 9 of Ref. [31] for voltage ratios).

0.5 and 1 (see the top of Fig. 7) for four-element lenses. In this case, the focusing power of the lens is determined by the ratios V_2/V_1 and V_3/V_1 , which can be larger or smaller than unity for a given voltage ratio V_4/V_1 . All parameters were determined firstly with fixed $V_4/V_1 = 5$ and then we also have given the results for different V_4/V_1 values.

Calculated values of the spherical and the chromatic aberration coefficient of the resulting zoom lens for a range of values of V_2/V_1 and V_3/V_1 are shown in Fig. 7. AB mode, for which the values of V_2/V_1 and V_3/V_1 are at a high voltage, has the lowest spherical and chromatic aberration coefficients and this is the better mode for using four-element lenses as a zoom lens. In the acceleration mode the electrons keep high energy all along their paths and stay generally much closer to the optical axis, and thus aberrations as well as the beam divergence are markedly reduced. Other cases have inherently higher aberration coefficients, essentially at the lower voltages (CD mode). When we compare the spherical and chromatic aberrations for two different values of A/D , it could be seen that the aberration coefficients for $A/D = 0.5$ is lower than $A/D = 1$, because of the different values of P and Q we used. The aberrations are lower for object positions closer to the reference plane, which is in agreement with the previous data [39]. On the other hand, the lens having $A/D = 1$ offers the advantage of a slightly wider range of magnifications and small aberrations (see Fig. 8 for $P/D = Q/D = 3$) compared with $A/D = 0.5$ for the same object and image distance.

In order to see the effects of the object and image distance on aberrations, we have calculated the spherical and chromatic aberration coefficients as a function of V_4/V_1 for six combinations of P , Q , and M as shown in Fig. 8. It is interesting to note that the increase in V_4/V_1 has the effect of reducing the aberration coefficients of the lens, and the minimums of C_s and C_c are significantly smaller than those of the previously mentioned three-element zoom lens. The four-element lens system shown in Fig. 7 has the advantage that a proper combination of P , Q and M can yield smaller aberration coefficients. Using these combinations it is possible to use a four-element lens as the spherical and chromatic aberration coefficients are then smaller for given focusing conditions, and these lower aberrations of the lens are quite noticeable. In addition, as V_4/V_1 increases, C_s and C_c become less sensitive to the lens voltages. This is desirable for obtaining a charged particle beam of a good quality, in a large range of final-to-initial electron energy. It is found that for large object–image distances ($P + Q$) both constant image position and magnification can be maintained with higher aberration coefficients. Especially, for $A/D = 1$ the field penetrations at the object and image positions are slightly larger than $A/D = 0.5$.

4.4. Five-element lenses

There are advantages in using multi-element lenses with more than four electrodes [40]. Some of the commonly used

configurations of five-element lenses are schematically shown in Fig. 9. As stated in the previous section, if a high positive voltage with respect to the first element's potential is applied to the lens elements, the aberrations as well as the minimum beam divergence can be reduced. The reason, obtained from numerical simulation, is that a positive voltage increases the electron velocity, shortening the electron drift time across the region with aberrant field. Therefore, it is of practical importance that the cases with

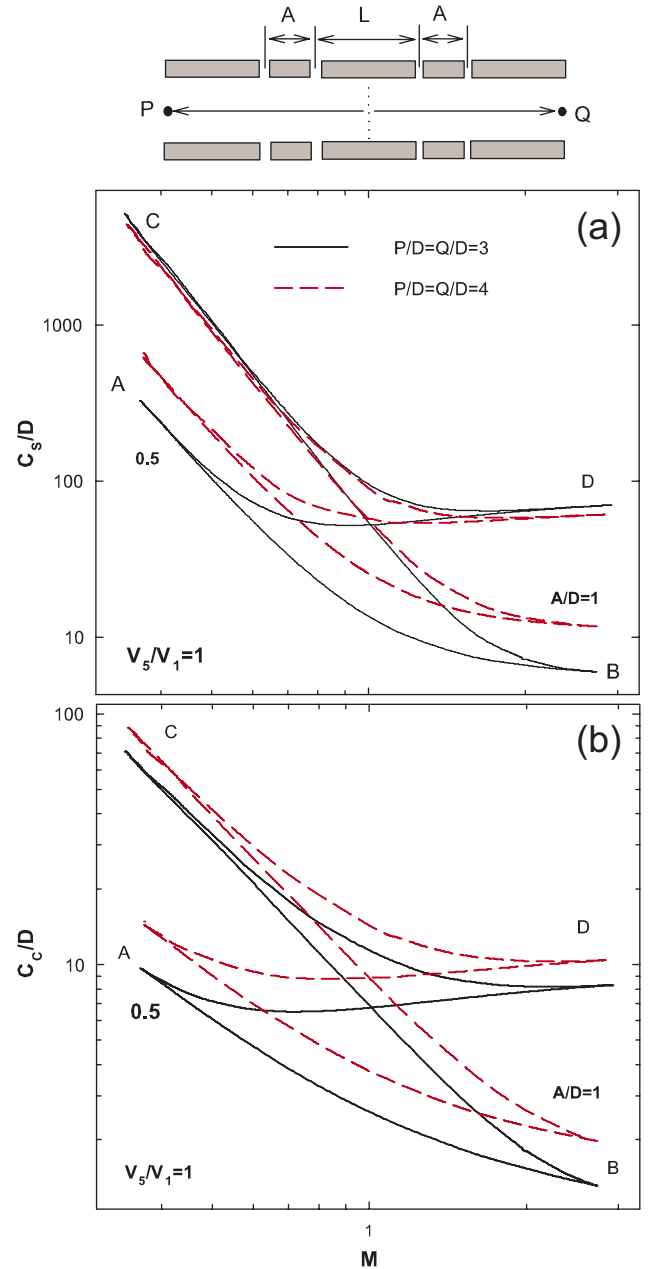


Fig. 9. (a) The spherical and (b) chromatic aberration coefficients, C_s/D and C_c/D , as a function of the magnification for $V_5/V_1 = 1$, and for $A/D = 0.5$ ($L/D = 2.5$) and 1 ($L/D = 3$) (see Fig. 12 of Ref. [31] for voltage ratios). For a given value of V_5/V_1 there are four pairs of values of V_2/V_1 and V_4/V_1 which satisfy the focusing condition: AB: $V_2/V_1 > 1$ and $V_4/V_1 > 1$; BC: $V_2/V_1 > 1$ and $V_4/V_1 < 1$; CD: $V_2/V_1 < 1$ and $V_4/V_1 < 1$; DA: $V_2/V_1 < 1$ and $V_4/V_1 > 1$.

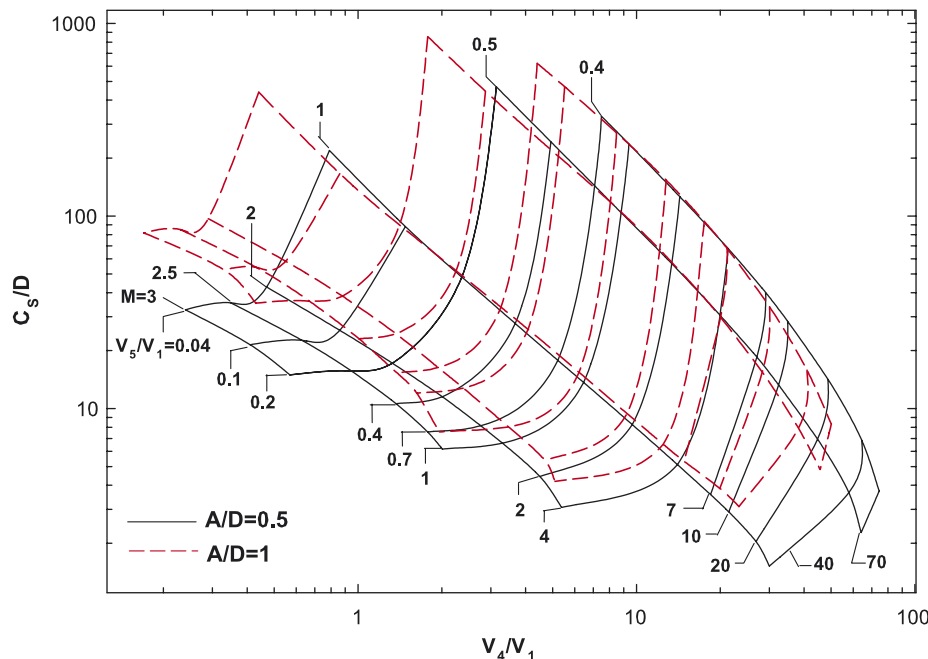


Fig. 10. The spherical aberration coefficients, C_s/D , as a function of V_4/V_1 in terms of the magnification M and V_5/V_1 for $A/D = 0.5$ ($L/D = 2.5$) and 1 ($L/D = 3$) (see Fig. 14 of Ref. [31] for voltage ratios).

$V_2/V_1 > 1$ and $V_4/V_1 > 1$ for five-element lenses have smaller aberration coefficients [41]. The other cases (as for example decelerating lenses) have higher spherical and chromatic aberrations. Some examples of calculated values of the spherical and chromatic aberration coefficients, C_s/D and C_c/D , are shown in Fig. 9 for $V_5/V_1 = 1$ and for two types of lens system $A/D = 0.5$ and 1. Similar curves can apply for other values of V_5/V_1 . In Fig. 10, we calculated the spherical aberration coefficient in terms of M and V_5/V_1 over a wide range that are especially convenient for low- and high-energy electron spectroscopy. These possible configurations of multi-element lenses imply that the variation in magnification and in aberration for an image point as for the cross-over could be controlled simultaneously [42].

5. Conclusions

This study sets out to simulate the aberration characteristics of multi-element electrostatic lenses in a form that can be verified and used by other electron optics designers and will make it relevant to spectrometers as well as electron beam applications. We have shown that by using the optimized voltages and geometry, the third order aberration coefficients of a lens system can be reduced significantly. In addition, the condition of higher energy at the center of the lens results in a lower aberration coefficient of the image. It is shown that the lens aberrations increase with increasing object and image distance, whereas field curvature decreases.

The effects of spherical aberrations on the intensity distribution in the final spot are also investigated. The first dominant part to the broadening of the line shape arises

from the spherical aberrations. It is independent of the beam energy for a constant voltage ratio. We found that spherical aberrations may be decreased by decreasing the maximum half angle, α_0 , correctly shaping the lenses and apertures, and adjusting the proper potential between the lens elements. The second part arises from the chromatic aberrations. This aberration plays an important role in low-energy electron beam applications. The comparison of focusing quality reported at the Gaussian image plane shows that the accelerating lens provides by far the best quality images.

Acknowledgments

The authors would like to express thanks to Theo J.M. Zouros for his help during the course of this study and A.R. Milosavljevic for carefully reading the manuscript. This work was supported by State Planning Organization in Turkey, through Grant 2002K120110 and Afyon Kocatepe University, Scientific Research Project Commission, through Grant 031-FENED-07.

References

- [1] P. Grivet, *Electron Optics*, Pergamon Press, London, 1965.
- [2] B. Paszkowski, *Electron Optics*, Iliffe, London, 1968.
- [3] O. Klemperer, M.E. Barnett, *Electron Optics*, third ed., Cambridge University Press, Cambridge, 1971.
- [4] E. Harting, F.H. Read, *Electrostatic Lenses*, Elsevier, Amsterdam, 1976.
- [5] M. Szilagy, *Electron and Ion Optics*, Plenum, New York, 1988.
- [6] P.W. Hawkes, E. Kasper, *Principles of Electron Optics*, vols. 1 and 2, Academic Press, London, 1989.

- [7] B. Lencová, Electrostatic lenses, in: J. Orloff (Ed.), Handbook of Charged Particle Optics, CRC Press, Boca Raton, 1997, pp. 177–221.
- [8] D.W.O. Heddle, Electrostatic Lens Systems, second ed., IOP Press, London, 2000.
- [9] J.N.H. Brunt, F.H. Read, J. Phys. E 8 (1975) 1015.
- [10] A. Renau, D.W.O. Heddle, J. Phys. E 19 (1985) 284.
- [11] A. Renau, D.W.O. Heddle, J. Phys. E 19 (1985) 288.
- [12] G. Martinez, M. Sancho, Nucl. Instr. and Meth. A 363 (1995) 198.
- [13] M. Szilagyi, Appl. Phys. Lett. 49 (1986) 767.
- [14] P.S. Vijayakumar, M. Szilagyi, Rev. Sci. Instr. 58 (1987) 953.
- [15] D. Olson, M. Szilagyi, Rev. Sci. Instr. 63 (1992) 3339.
- [16] O. Scherzer, Z. Phys. 101 (1936) 593.
- [17] I.C. Dowker, F.H. Read, N.J. Bowring, P. Hammond, Nucl. Instr. and Meth. A 363 (1995) 54.
- [18] L.A. Baranova, S.Ya. Yavor, Tech. Phys. 42 (1997) 938.
- [19] L.A. Baranova, F.H. Read, Int. J. Mass Spect. 189 (1999) 19.
- [20] L.A. Baranova, F.H. Read, Optik 112 (2001) 131.
- [21] L.A. Baranova, F.H. Read, D. Cubric, Nucl. Instr. and Meth. A 519 (2004) 42.
- [22] M. Kato, T. Sekine, J. Vac. Sci. Technol. A 13 (1995) 2255.
- [23] M. Kato, T. Sekine, J. Vac. Sci. Technol. A 14 (1997) 453.
- [24] H. Matsuda, H. Daimon, M. Kato, M. Kudo, Phys. Rev. E 71 (2005) 1.
- [25] S. Uno, K. Honda, N. Nakamura, M. Matsuya, J. Zach, Optik 116 (2005) 438.
- [26] C.E. Kuyatt, D. DiChio, S.V. Natali, J. Vac. Sci. Technol. A 10 (1973) 1124.
- [27] K. Saito, T. Okubo, K. Takamoto, Y. Uno, M. Kondo, J. Vac. Sci. Technol. A 4 (1986) 1913.
- [28] Z. Liu, Ultramicroscopy 117 (2005) 196.
- [29] D.A. Dahl, SIMION 3D v7.0, Idaho National Engineering Laboratory, Idaho Falls, 1996.
- [30] CPO programs, free version available from (www.electronoptics.com).
- [31] O. Sise, M. Ulu, M. Dogan, Nucl. Instr. and Meth. A 554 (2005) 114.
- [32] M. Dogan, A. Crowe, K. Bartschat, P.J. Marchalant, J. Phys. B 31 (1998) 1611.
- [33] T.J.M. Zouros, O. Sise, F.M. Spiegelhalter, D.J. Manura, Int. J. Mass Spectro, in print, 2006. (<http://dx.doi.org/10.1016/j.ijms.2006.08.005>). (See also <http://www.simion.com/tools/sc>).
- [34] P.W. Hawkes, B. Lencova, Optik 2 (2002) 78.
- [35] M. Bernheim, Ultramicroscopy 106 (2005) 398.
- [36] K.J. Harte, J. Vac. Sci. Technol. 10 (1973) 1098.
- [37] A.R. Milosavljevic, et al., Meas. Sci. Technol. 16 (2005) 1997.
- [38] F.H. Read, J. Phys. E 5 (1971) 156.
- [39] G. Martinez, M. Sancho, F.H. Read, J. Phys. E 16 (1983) 631.
- [40] D.W.O. Heddle, N. Papadovassilakis, J. Phys. E 17 (1984) 599.
- [41] C. Trager-Covan, S.M. Kay, D.W.O. Heddle, Meas. Sci. Technol. 1 (1990) 738.
- [42] R.A. Colman, G.J.F. Legge, Nucl. Instr. and Meth. B 84 (1994) 515.